

Supporting Information

Chromium (III)-Doped Phosphors of High-Efficiency Two-Site Occupation Broadband Infrared Emission for Vessel Visualization Applications

Guohui Wei, Panlai Li*, Rui Li, Jiehong Li, Yawei Shi, Ye Wang, Shaoxuan He, Yuanbo Yang, Hao Suo, Zhijun Wang*

Hebei Key Laboratory of Optic-electronic Information and Materials, College of Physics Science & Technology, Hebei University, Baoding 071002, China

Corresponding authors

E-mail: *li_panlai@126.com

E-mail: *wangzj1998@126.com

Experimental Section

Materials and preparation: Powder samples were prepared by the conventional air-solid phase method using $\text{Mg}_7\text{Ga}_2\text{GeO}_{12}: x\text{Cr}^{3+}$ ($0 \leq X \leq 0.15$) as the constituents. The initial materials for chemical statistics include MgO (99.99%, Aladdin), Ga_2O_3 (99.99%, Aladdin), In_2O_3 (99.99%, Aladdin), Li_2CO_3 (99.99%, Aladdin), H_3BO_3 (1 % Li_2CO_3 and 3 % H_3BO_3 as co-solvent contribute to grain growth), GeO_2 (AR) and Cr_2O_3 (99.95%, Aladdin), were weighed according to the given stoichiometric ratio, mixed, and ground uniformly in an agate mortar for 30 min. The mixture was then transferred to a corundum crucible and placed in a muffle furnace and sintered at 1500°C for 6 h. Finally, the furnace was naturally cooled to room temperature and the samples were ground to a fine powder for subsequent characterization.

Characterization: The X-ray diffractograms were tested with a Bruker D8 Advance X-ray diffractometer under $\text{Cu-}\alpha$ ($\lambda=1.54056\text{\AA}$) irradiation at 40 kV and 40 mA. The morphological characteristics of the prepared phosphors were recorded with a field emission scanning electron microscope (Nova Nano SEM 450). Rietveld refinement of the measured XRD data was performed using GSAS software. The spectra were recorded with a HORIBA FLuorolog 3 fluorescence spectrometer. Diffuse reflectance spectra were measured by a Hitachi U4100. Electron spin resonance (EPR) measurements were performed on a 100 K EPR spectrometer (Bruker, A300). XPS was obtained using an X-ray photoelectron spectrometer (ThermoFisher ESCALAB 250Xi).

LED performance: The NIR LED devices were made of synthetic NIR phosphor and blue light chips emitting 450 nm. the mass ratio of AB glue and NIR phosphor was set to 1:1 and mixed uniformly. The night vision pictures taken were obtained with the aid of an industrial night vision camera.

Table S1 Ga_x/Mg_x (x=1, 2, 3, 4) bond lengths, bond mean lengths, and torsion resistance.

	D₁₋₄ (Å)	D₅ (Å)	D₆ (Å)	Mean length (Å)	Torsion (σ)	resistance
Mg₁/Ga₁	2.088	2.120	2.120	2.099		0.014
Mg₂/Ga₂	2.088	2.122	2.122	2.099		0.015
Mg₃/Ga₃	2.088	2.122	2.120	2.099		0.014
Mg₄/Ga₄	2.088	2.120	2.122	2.099		0.014

Table S2 Refined crystallographic data of $\text{Mg}_7\text{Ga}_{2-x}\text{GeO}_{12-x}\text{Cr}^{3+}$ ($x=0-0.15$).

x	0	0.01	0.03	0.05	0.07	0.09	0.11	0.13	0.15
Crystal System	Orthorhombic								
Space group	Cmmm								
a (Å)	5.8509	5.8499	5.8500	5.8502	5.8506	5.8496	5.8476	5.8504	5.8494
b (Å)	25.4547	25.4550	25.4547	25.4549	25.4581	25.4567	25.4492	25.4596	25.4552
c (Å)	2.9822	2.9817	2.9818	2.9819	2.9820	2.9815	2.9805	2.9819	2.9816
Z	2								
Cell Volume (Å³)	444.143	443.998	444.007	444.017	444.016	443.980	443.541	444.054	443.984
R_{WP} (%)	9.38	9.52	9.32	9.28	9.53	9.14	9.69	9.53	9.47
R_p (%)	6.72	6.84	6.50	6.50	6.84	6.53	6.79	6.75	6.86
χ²	2.540	2.592	2.495	2.468	2.564	2.364	2.588	2.476	2.541

Table S3 The D_q/B value calculated from the excitation spectra of Mg₇Ga_{2-x}GeO₁₂:xCr³⁺ (x=0.01-0.13).

x	⁴ A ₂ → ⁴ T ₂ (⁴ F)	⁴ A ₂ → ⁴ T ₁ (⁴ F)	D _q /B
0.01	442 nm	620 nm	2.48
0.05	438 nm	619 nm	2.39
0.07	440 nm	618 nm	2.45
0.09	441 nm	619 nm	2.43
0.11	438 nm	618 nm	2.41
0.13	440 nm	622 nm	2.38

Table S4 Luminescent parameters of Mg₇Ga_{1.91-y}GeO₁₂:0.09Cr³⁺, yIn³⁺ with In³⁺ concentrations.

Y	0	0.01	0.03	0.05	0.07	0.09	0.11
IQE (%)	51.261	53.109	59.892	70.476	85.869	76.86	66.297
EQE (%)	15.309	15.855	19.551	29.379	37.8	33.369	24.297
AE (%)	29.86	30.1	33.65	42.5	44.23	43.13	38.118

Measurements of quantum efficiency

The photoluminescence quantum efficiency was recorded with a HORIBA FLuorolog3 fluorescence spectrometer, and the low-temperature spectra were tested with an external device using a 450W Xe lamp as the excitation source. BaSO₄ was used as a standard reference. Spectral test range 240-1700 nm, quantum efficiency test range 240-850 nm. The quantum efficiency (QE) measurement was performed at room temperature by using a HORIBA FLuorolog3 fluorescence spectrometer with a 450W Xe lamp. The internal quantum efficiency (IQE) is defined as the percentage of the number of emitted photons to that of absorbed photons, which can be calculated using the following equation:

$$IQE = \frac{\int L}{\int E_R - \int E_S} \times 100\% \quad (1)$$

L is the luminescence spectrum of the sample, E_S is the excitation spectrum of the sample, and E_R is the excitation spectrum referenced by BaSO₄. In addition, the external quantum efficiency (EQE) is

defined as the percentage of the number of emitted photons to the number of exciting photons:

$$EQE = \frac{\int L}{\int E_R} \times 100\% \quad (2)$$

The absorption efficiency (AE) is defined as the percentage of the number of absorbed photons (by the sample) to that of excitation photons:

$$AE = \frac{\int E_R - E_S}{\int E_R} \times 100\% \quad (3)$$

Table S5 The luminescence properties of some broadband NIR phosphors.

Phosphor	Em (nm)	Fwhm (nm)	IQE/EQE
La₂MgZrO₆:Cr³⁺	825nm	210nm	58%/-
Ca₂LuHf₂AlO₁₂:Cr³⁺	785nm	145nm	-/-
Na₃ScF₆:Cr³⁺	774nm	108nm	91.5%/40.82%
ScBO₃:Cr³⁺	800nm	120nm	65%/-
Ca₃Sc₂Si₃O₁₂:Cr³⁺	770nm	140nm	92.3/-
LiScGeO₄:Cr³⁺	1100nm	335nm	-/-
ScF₃:Cr³⁺	853nm	140nm	45%/-
MgAl₂O₄:Cr³⁺	740nm	140nm	15%/-
LiScP₂O₇:Cr³⁺	880nm	170nm	74%/-
Mg₇Ga₂GeO₁₂:Cr³⁺, In³⁺	850nm	266nm	86%/37%

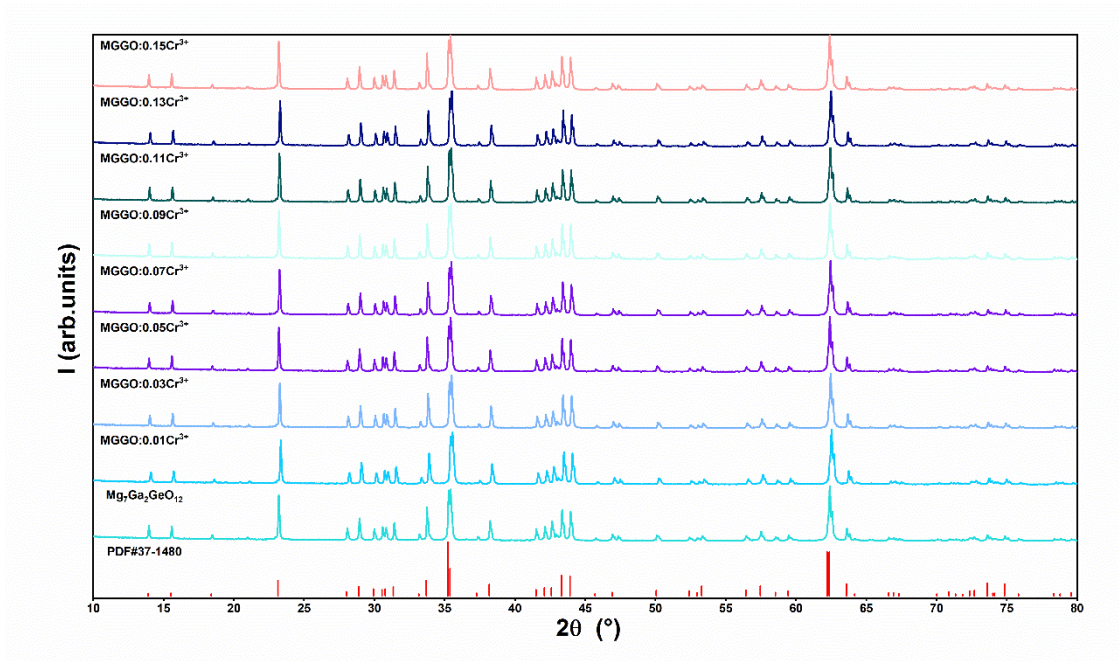


Figure S1 XRD of $\text{Mg}_7\text{Ga}_{2-x}\text{GeO}_{12}:x\text{Cr}^{3+}$ ($x=0.01-0.15$).

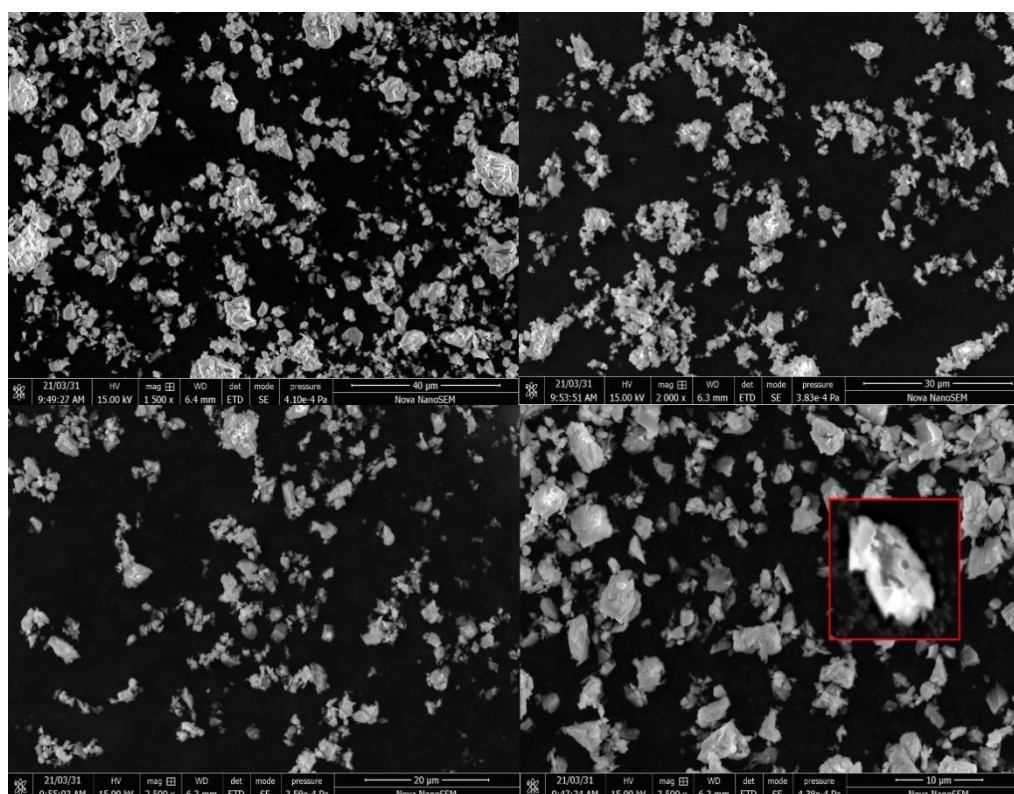


Figure S2 SEM of $\text{Mg}_7\text{Ga}_{1.91}\text{GeO}_{12}:0.09\text{Cr}^{3+}$.

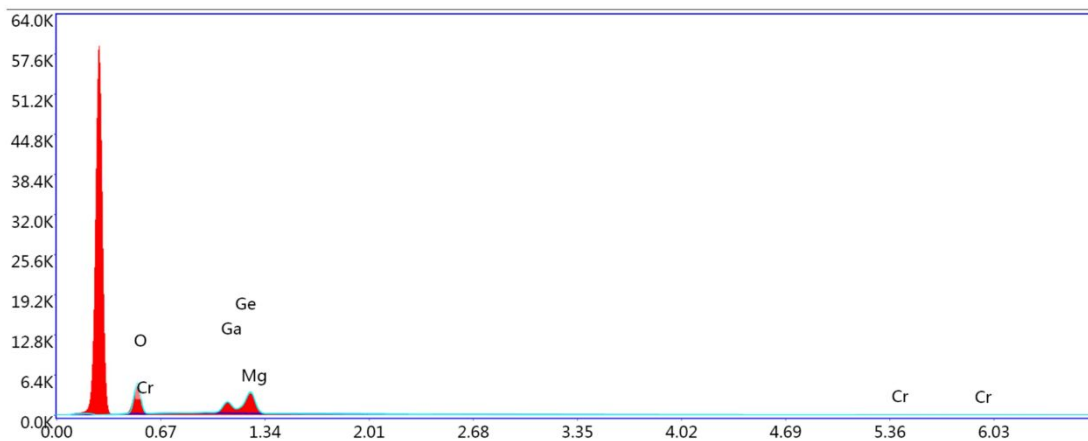


Figure S3 EDS of $\text{Mg}_7\text{Ga}_{1.91}\text{GeO}_{12}:0.09\text{Cr}^{3+}$.

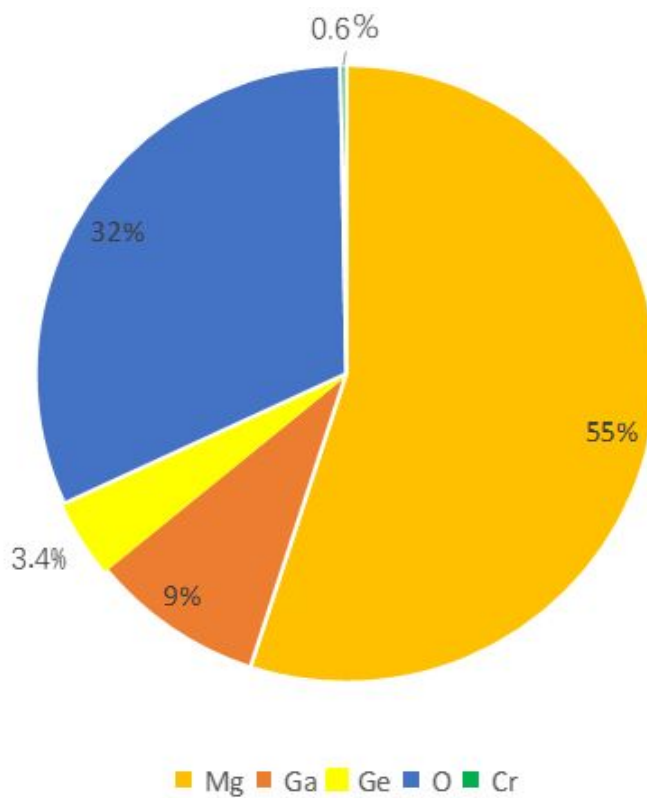


Figure S4 Content ratio of each element of $\text{Mg}_7\text{Ga}_{1.91}\text{GeO}_{12}:0.09\text{Cr}^{3+}$.

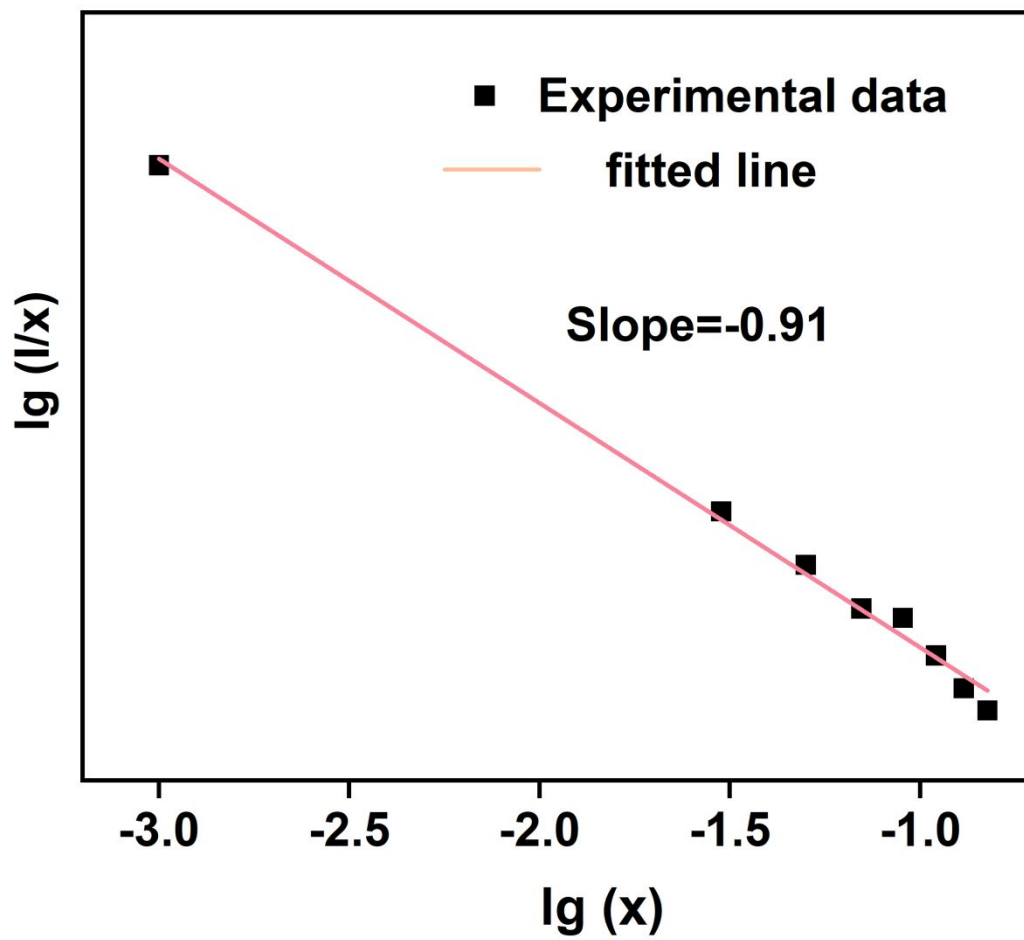


Figure S6 Linear relationship between $lg(I/x)$ and $lg(x)$.

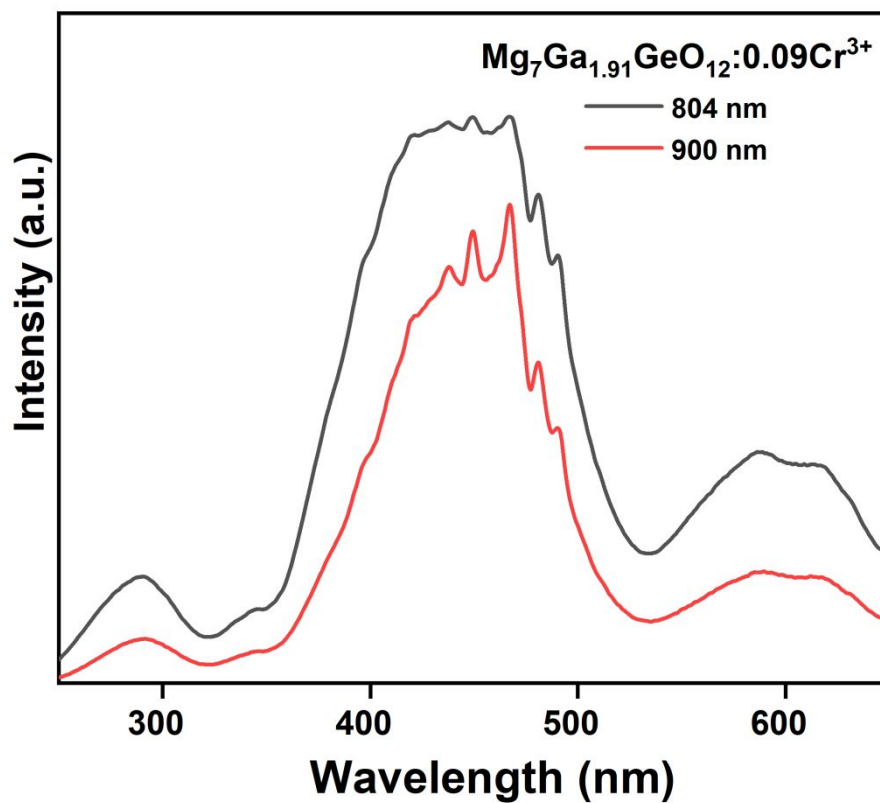


Figure S7 Excitation spectra of $\text{Mg}_7\text{Ga}_{1.91}\text{GeO}_{12}:\text{0.09Cr}^{3+}$ ($\lambda_{\text{em}}=804$ nm and 900 nm).

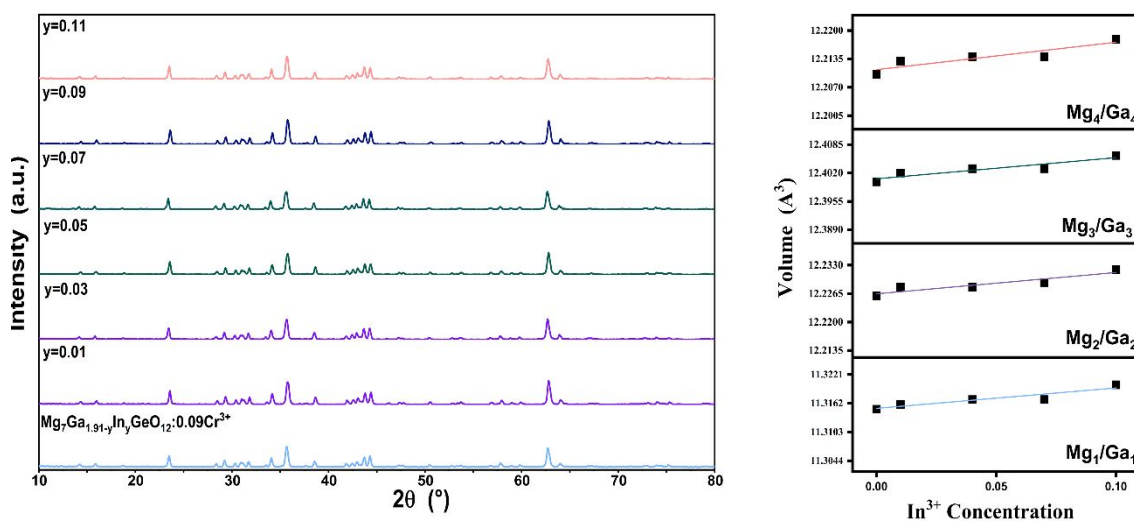


Figure S8 XRD patterns of $\text{Mg}_7\text{Ga}_{1.91-y}\text{In}_y\text{GeO}_{12}:\text{0.09Cr}^{3+}$ ($y=0.01-0.11$) and the trend of volume change of Mg_x/Ga_x ($x=1, 2, 3, 4$) hexahedron.

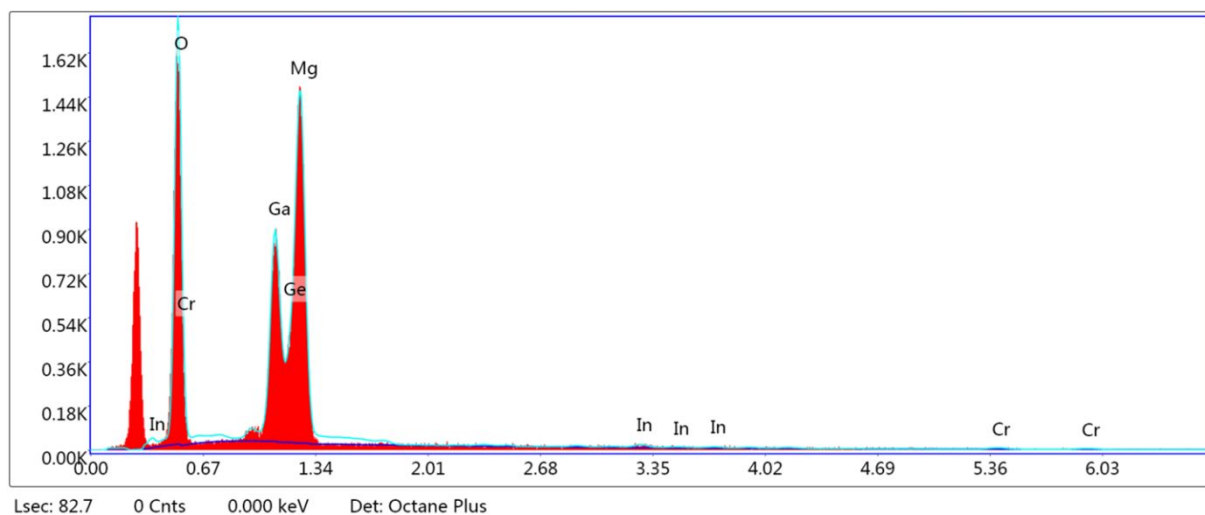


Figure S9 Content ratio of each element of $\text{MgIn}_{0.07}\text{GO}:0.09\text{Cr}^{3+}$.

Element	Weight %	Atomic %	Net Int.	Error %	K ratio	Z	A	F
O K	28.5	49.7	228.8	5.1	0.2377	1.0701	0.7786	1.0000
Ga L	27.7	11.1	118.0	4.2	0.2211	0.7474	1.0675	1.0008
Ge L	10.8	4.1	41.3	8.1	0.0773	0.7381	0.9735	1.0004
Mg K	29.3	33.6	247.2	5.3	0.2251	0.9869	0.7788	1.0001
In L	1.9	0.5	3.0	50.6	0.0130	0.6704	1.0184	1.0005
Cr K	1.9	1.0	1.8	62.7	0.0163	0.8401	0.9995	1.0461

Figure S10 Content ratio of each element of $\text{Mg}_7\text{Ga}_{1.84}\text{In}_{0.07}\text{GeO}_{12}:0.09\text{Cr}^{3+}$.

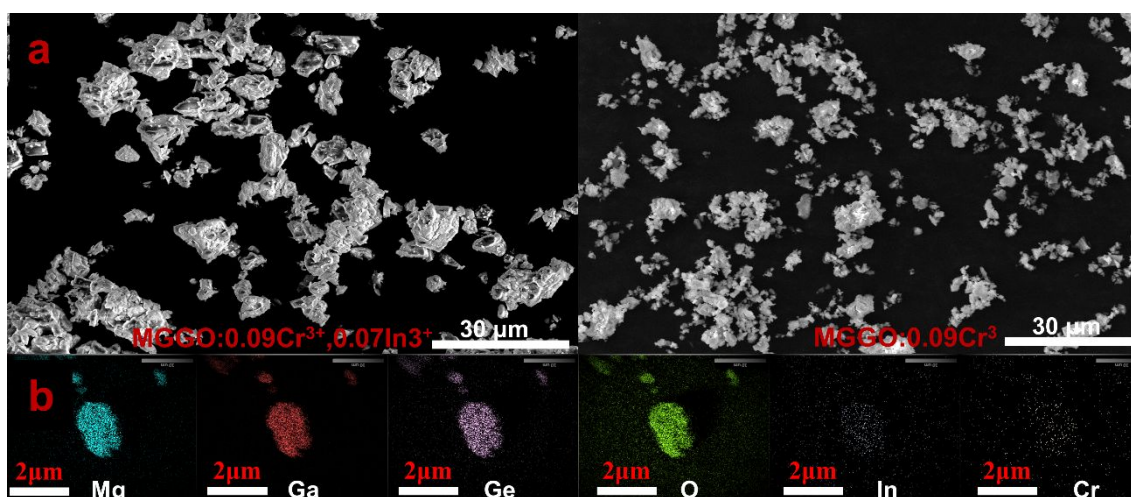


Figure S11 SEM and Mapping of $\text{Mg}_7\text{Ga}_{1.84}\text{In}_{0.07}\text{GeO}_{12}:0.09\text{Cr}^{3+}$ and $\text{Mg}_7\text{Ga}_{1.91}\text{GeO}_{12}:0.09\text{Cr}^{3+}$.

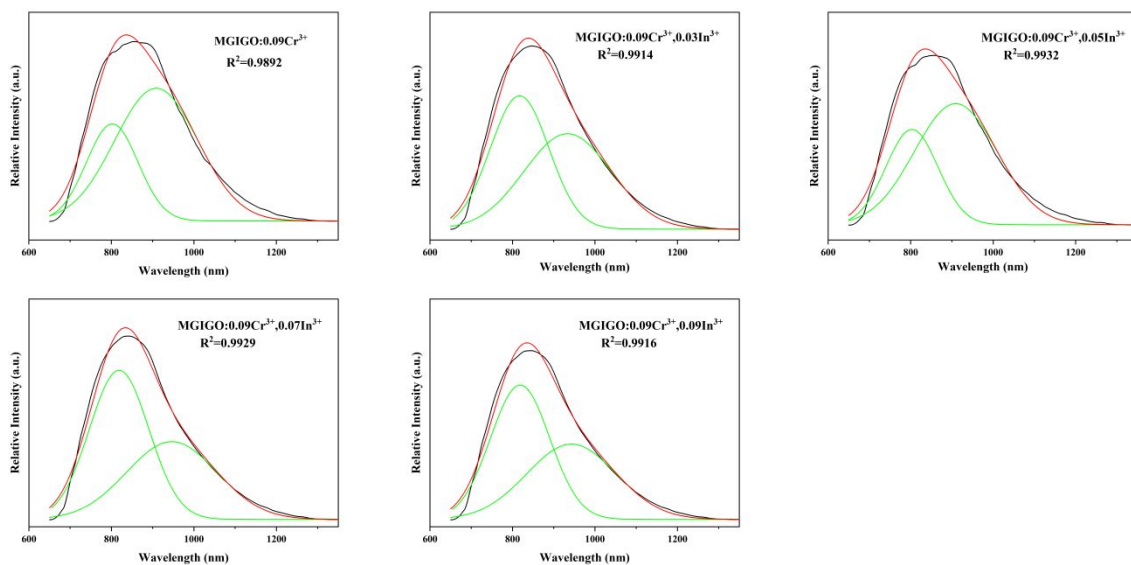


Figure S12 Gaussian fitting for PL spectra of $\text{MGI}_y\text{GO}:0.09\text{Cr}^{3+}$ ($0 \leq y \leq 0.11$) ($\lambda_{\text{ex}}=442$ nm).

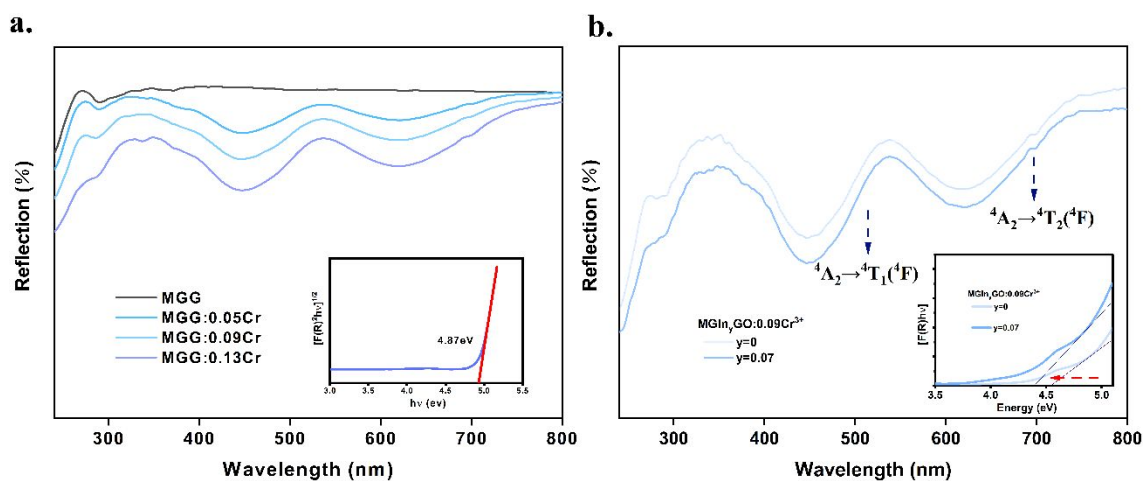


Figure S13 a. Diffuse reflection spectrum of $\text{Mg}_7\text{Ga}_{2-x}\text{GeO}_{12}:x\text{Cr}^{3+}$ ($x = 0, 0.05, 0.09, 0.13$), inset: band gaps of $\text{Mg}_7\text{Ga}_{2-x}\text{GeO}_{12}$. **b.** Diffuse reflection spectra of $\text{Mg}_7\text{Ga}_{1.91-y}\text{In}_y\text{GeO}_{12}:0.09\text{Cr}^{3+}$ ($y = 0, 0.01, 0.07$ and 0.11), inset: band gaps of $\text{Mg}_7\text{Ga}_{1.91-y}\text{In}_y\text{GeO}_{12}:0.09\text{Cr}^{3+}$ ($y = 0$, and 0.07).

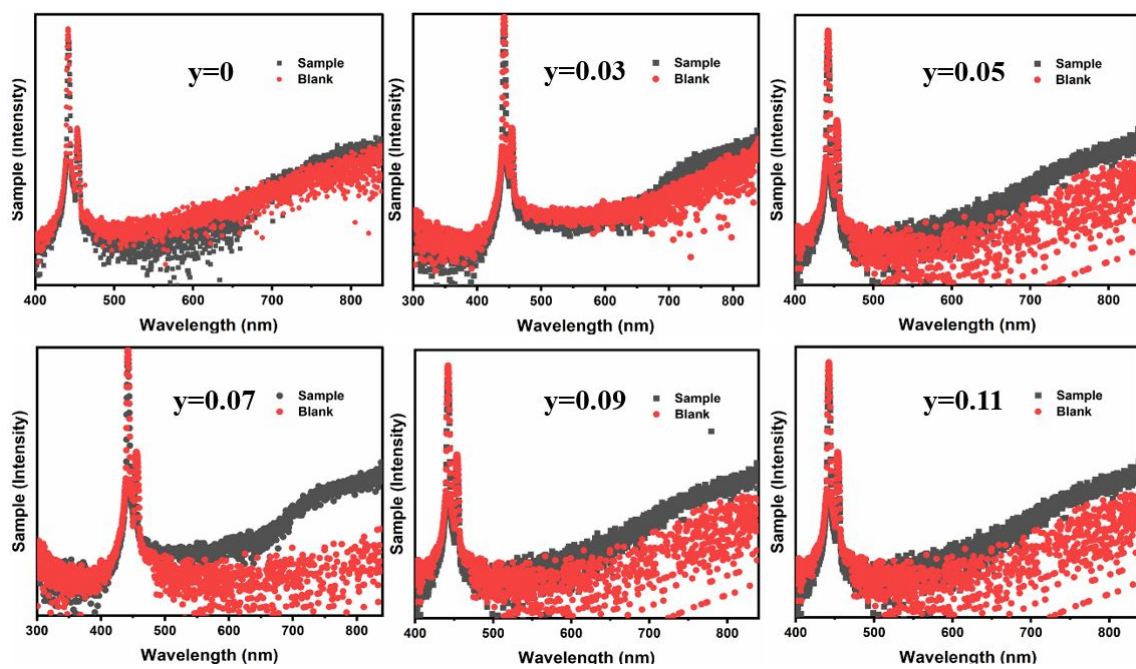


Figure S14 The luminescent spectra for the IQE of $\text{Mg}_7\text{Ga}_{1.91-y}\text{In}_y\text{GeO}_{12}:0.09\text{Cr}^{3+}$ ($y=0, 0.03, 0.05, 0.07, 0.09, 0.11$).

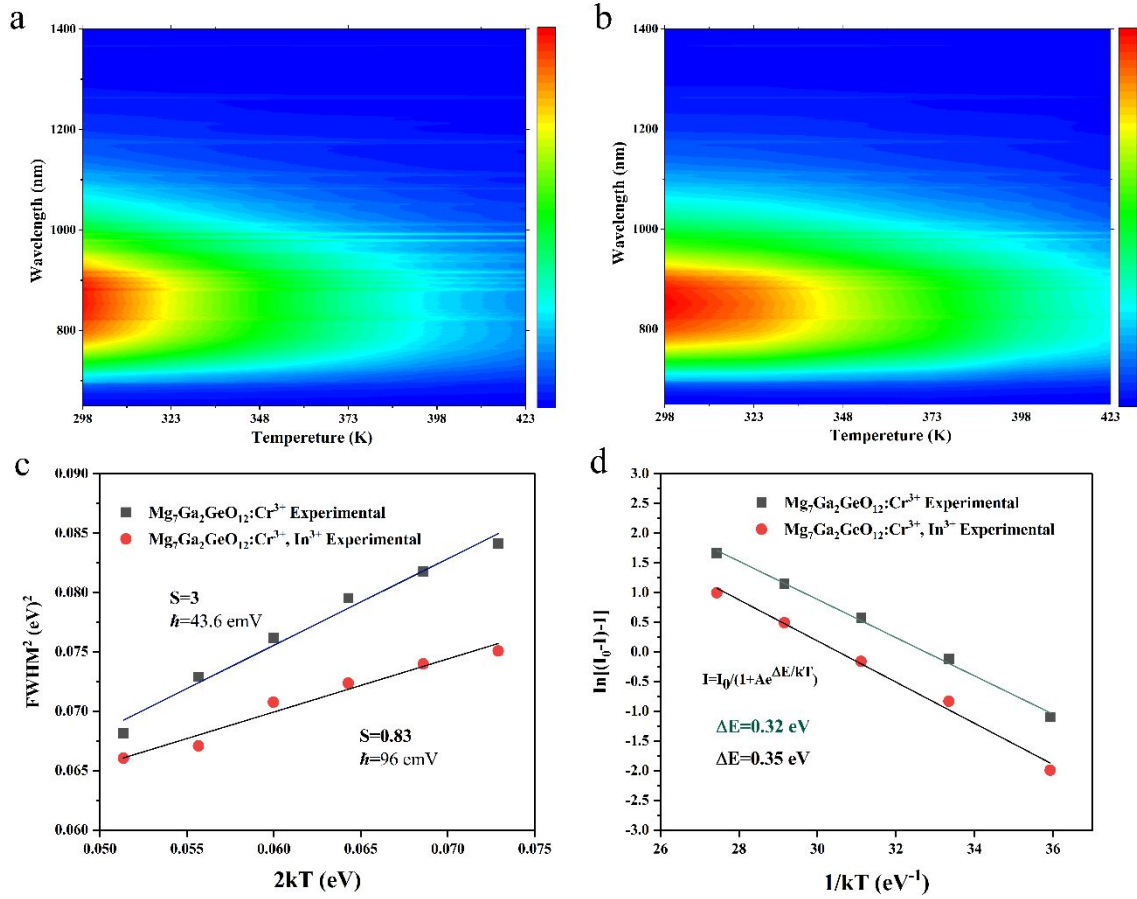


Figure S15 ab. Temperature-dependent PL spectra of samples $\text{Mg}_7\text{Ga}_{1.91-y}\text{In}_y\text{GeO}_{12}:0.09\text{Cr}^{3+}$ ($y=0, 0.07$). c. Fitting results of FWHM^2 as a function $2kT$. d. Fitting results of $\ln[(I_0-I)^{-1}]$ as a function $2kT$. The values are the fitting result for the Arrhenius equation of $\text{Mg}_7\text{Ga}_{1.91}\text{GeO}_{12}:0.09\text{Cr}^{3+}$, and $\text{Mg}_7\text{Ga}_{1.91}\text{GeO}_{12}:0.09\text{Cr}^{3+}, 0.07\text{In}^{3+}$.